J. Phys.: Condens. Matter **9** (1997) 381–387. Printed in the UK PII: S0953-8984(97)76005-3

Isostructural solid–solid transitions in systems with a repulsive 'shoulder' potential

Peter Bolhuis and Daan Frenkel

FOM Institute for Atomic and Molecular Physics, Kruislaan 407, 1098 SJ Amsterdam, The Netherlands

Received 5 July 1996

Abstract. Using Monte Carlo simulations, we study the phase behaviour of systems with a short-ranged repulsive 'shoulder' potential. In analogy to systems with a short-ranged attractive interaction, the shoulder potential leads to an isostructural solid–solid phase transition. We show that the range of interactions for which a solid–solid transition is possible is much wider for repulsive than for attractive interactions.

It is well known that weak, long-ranged attractive intermolecular forces lead to a liquid–vapour transition (see e.g. [1]). Recently, we considered the opposite limit of attractions that act over distances that are small compared to the hard-core radius of the particles [2]. Such interaction can occur in certain colloidal systems. We found that a dense system of spherical particles with very short-ranged interaction may exhibit a solid–solid transition that is in many ways reminiscent of the liquid–vapour transition. In particular, the transition takes place between two phases that have the *same* structure. And secondly, the line of (first-order) solid–solid transitions ends in a critical point. We found that the critical density depends strongly on the range of the intermolecular interaction. In the square-well model considered in reference [2] the solid–solid critical point crosses the melting curve if the range of attraction is more than 6% of the hard-core diameter. The critical temperature is much less sensitive to the range of attraction.

Subsequent theoretical studies support the existence of such behaviour for a variety of models [3–6], even though, thus far, direct experimental observation of this solid–solid transition is lacking. However, one of the predicted consequences of the vicinity of a solid–solid transition in two dimensions is the stabilization of the hexatic phase [7], and recent experiments by Marcus and Rice [8] seem to support this scenario.

An isostructural solid–solid transition can also take place in systems involving only repulsive interactions. It is known that isostructural solid–solid transitions can occur in dense Cs and Ce [9]. These transitions are believed to be due to the softness of the intermolecular potential associated with a pressure-induced change in the electronic state of the metal ions. Theoretical work by Stell and Hemmer [10], and simulations by Alder and Young [11] indicate that such softness may indeed result in a solid–solid transition. Kincaid, Stell and Goldmark [12] modelled the interaction potential of such systems by a so-called square shoulder (a hard-sphere potential augmented with a repulsive plateau) and calculated the phase behaviour by applying perturbation theory. In this paper we compute the phase behaviour of a system of spherical particles interacting via a square-shoulder potential. The difference from earlier work is that we focus on a relatively short-ranged shoulder potential.

Hence the model that we consider is the repulsive counterpart of the narrow-square-well model studied in reference [2]. Such short-ranged repulsive interactions may occur in a variety of colloidal and macro-molecular systems. A possible example is a colloid that is sterically stabilized by partly interpenetrable layers of grafted chain molecules.

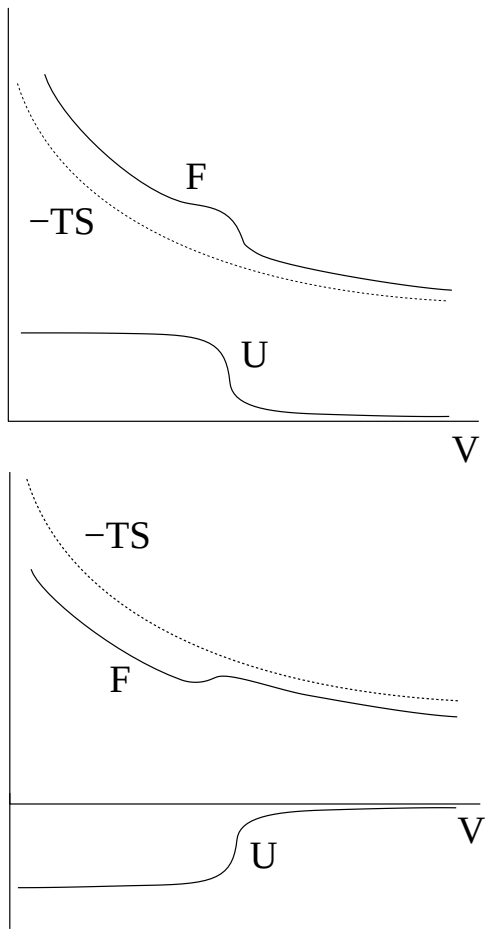

Figure 1. A rough sketch of the influence of the rapid change in the potential energy U on the total free energy $F = U - TS$. The top figure shows the situation for the square-shoulder case, whereas the bottom figure refers to a square-well system. All curves are plotted as functions of the system volume V.

Kincaid, Stell and Goldmark [12] studied the phase behaviour of spheres with a short-ranged repulsive interaction potential of the form

$$v(r) = \begin{cases} \infty & 0 \leqslant r < \sigma \\ \epsilon & \sigma \leqslant r < \sigma + \delta \\ 0 & r \geqslant \sigma + \delta \end{cases} \tag{1}$$

where σ is the diameter of the spherical particle and ϵ is the height of the repulsive shoulder. Using perturbation theory, Kincaid *et al* calculated the isostructural solid–solid phase transition in this kind of system. Basically, the mechanism of this phase transition is the same as for the square-well model as described in reference [2]. A first-order phase

transition takes place if there is an inflection point in the free energy as a function of volume. The free energy is the sum of the potential energy U and an entropy term $-TS$. We know that this entropy term (or equivalently the free energy of a reference hard-sphere system with diameter σ) is a monotonically decreasing function of the volume. For the square-well system the potential energy increases slowly with volume, suddenly rises steeply when the average distance between the particles approaches the well width, and levels off again for lower densities. At low enough temperatures the total free energy will show the inflection point which is indicative of a first-order phase transition, as is illustrated in figure 1.

In the case of the square-shoulder systems the potential energy decreases with volume. However, as the volume increases beyond the point where the shoulders begin to overlap, the potential energy will first decrease steeply and then level off. At low enough temperature this variation of the potential energy will also lead to an inflection point in the volume dependence of the free energy, as is shown in figure 1. There are, of course, differences from the square-well case. First of all, for the same range of interaction, the inflection point of the free energy, and hence the critical point will occur at higher densities. The other major difference will be at low temperatures. For the square-well potential, the low-density solid is only stable above the triple-point temperature (and disappears completely when the range of attraction exceeds 6% of the hard-core diameter). In contrast, for the repulsive shoulder potential, the expanded solid is stable in the low-temperature limit. Once the solid–solid critical point crosses the melting curve, we expect that the expanded solid phase will only exist as an isolated solid pocket in the liquid phase. This is reminiscent of the behaviour considered in a model proposed by Poole *et al* [13] to account for the phase behaviour of supercooled water.

In order to compute the phase diagram of the square-shoulder system, we first must determine the dependence of the Helmholtz free energy of the solid on density and temperature. We use thermodynamic integration to relate the free energy of the square-shoulder solid to that of a reference hard-sphere solid at the same density (see e.g. [15]):

$$F(\rho, \epsilon^*) = F_{HS}(\rho) + \int \mathrm{d}\epsilon^* \left(\frac{\partial F}{\partial \epsilon^*}\right) = F_{HS}(\rho) + \int \mathrm{d}\epsilon^* \, \frac{\langle U \rangle_{\epsilon^*}}{\epsilon^*} \tag{2}$$

where $\epsilon^* = \epsilon / k_B T$ is the reduced shoulder height, $\rho = N/V$ is the number density and $\langle U \rangle$ is the average potential energy of the system. The instantaneous potential energy is equal to the number of pairs of atoms N_p that are within the range of the potential times the height of the potential shoulder ϵ. The dimensionless free energy per particle now is simply

$$\frac{F(\rho, \epsilon^*)}{N k_B T} = \frac{F_{HS}(\rho)}{N k_B T} - \int \mathrm{d}\epsilon^* \, \frac{\langle N_p \rangle_{\epsilon^*}}{N}. \tag{3}$$

The free energy of the three-dimensional hard-sphere solid F_{HS} is well known and can be accurately represented using the analytical form for the equation of state proposed by Hall [16]. The presence of a first-order phase transition in the square-shoulder solid is signalled by the fact that the Helmholtz free energy becomes a non-convex function of the volume. The densities of the coexisting phases can then be determined by a standard double-tangent construction.

In order to map out the phase diagram of the square-shoulder solid over a wide range of densities and temperatures as a function of the width of the repulsive shoulder, several thousand independent simulations were required. To keep the computational costs within bounds, we chose to simulate a relatively small system. With a small system size, finite-size effects are expected, in particular in the vicinity of a critical point. However, away from critical points finite-size effects should be so small that they will not affect the conclusions

that we draw below. In what follows, we use reduced units, such that ϵ/k_B is the unit of temperature, and σ, the hard-core diameter of the particles, is the unit of length.

All simulations on the three-dimensional system were performed on a face-centred cubic (fcc) solid consisting of 108 particles. This is presumably the stable solid structure for hard spheres at high density and also for hard spheres with a narrow shoulder potential. In fact, for hard spheres, the difference in free energy of the face-centred cubic and hexagonal close-packed (hcp) structures is so small that it is not known which one is the more stable. Our calculations were performed for the fcc structure, but the results would have been virtually the same for the hcp structure. Other crystal structures (e.g. simple cubic and body-centred cubic, bcc) can be ignored at densities above $\rho = 1.3$, because they have a lower maximum packing density. At lower densities, other solid phases could be stable, at least in principle. In fact, very recent calculations of Mederos *et al* on a system with a shoulder potential width of $\delta = 0.1$ suggest that the bcc crystal structure may be stable at low temperature and densities smaller than $\rho = 1.1$ [14].

The simulation box was chosen to be cubic and periodic boundaries were applied. The densities ranged from $\rho = 0.9$ which is below the hard-sphere melting point to $\rho = 1.414$ which is almost at close packing ($\rho_0 = \sqrt{2}$). The temperature of the system was varied in the range $0 < 1/T < 2$, in steps of 0.1. Simulations were performed for $\delta = 0.00$, 0.01, 0.02, 0.03, 0.04, 0.05, 0.06, 0.07 and 0.08. For every value of the shoulder width δ we performed some 1000 MC simulations of 20 000 cycles each.

In order to perform the double-tangent construction on the Helmholtz free energy, all simulation data were fitted to an analytical function of ρ, δ and T. We chose to use a fit function that reproduced the correct limiting behaviour at close packing. In particular, we used the following functional form:

$$N_p(\delta, T^{-1}, x)/N = 3 + 3\,\mathrm{erf}(x-1) + \mathrm{e}^{-2x+5} \sum_{i,j,k=0}^{1,2,6} c_{ijk}\delta^i T^{-j} x^k. \tag{4}$$

The parameter x in equation (4) is defined as the ratio of shoulder width d to the distance a that characterizes the expansion of the solid from close packing: $a \equiv r_{nn} - \sigma$, where r_{nn} is the average nearest-neighbour distance. x is simply related to the density, through

$$x = \frac{\delta}{a} = \frac{\delta}{(\rho_0/\rho)^{1/3} - 1}. \tag{5}$$

For large x—i.e. near close packing—the value of the function in equation (4) approaches half the number of nearest neighbours per particle.

Table 1. Best-fit coefficients c_{ijk} for equation (4).

		k						
i	j	0	1	2	3	4	5	6
0	0	13.442	−29.520	26.414	−12.292	3.128	−0.412	0.022
0	1	−104.645	231.297	−206.447	95.183	−23.950	3.127	0.165
0	2	98.844	−226.082	209.598	−2191.837	26.472	−3.612	0.200
1	0	−291.152	692.956	−677.704	348.211	−99.113	14.811	−0.907
1	1	1861.480	−4408.039	4287.814	−100.732	620.43	−92.139	5.606
1	2	−1218.127	2865.821	−2775.223	1415.943	−401.124	59.750	−3.652

The coefficients of the best fits to the numerical data are given in table 1. These fits reproduce the numerical data to within the statistical error. Using the functional forms given

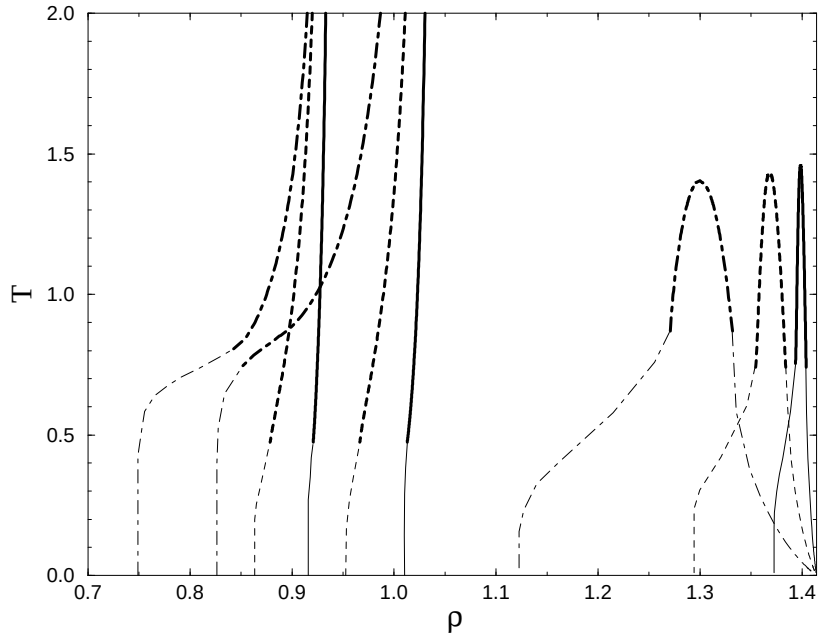

Figure 2. Computed phase diagrams in the T, ρ plane for the fcc structure of 108 square-shoulder particles. The solid curves correspond to shoulder width $\delta = 0.01$, the dashed curves to $\delta = 0.03$ and the chain curves to $\delta = 0.08$. The thick curves indicate simulation results. The thin curves are extrapolations to the exact results at $T = 0$.

by equation (4) to represent the numerical data, we computed the free energy of the solid as a function of temperature and volume, using equation (3). The resulting free-energy functions were checked for possible non-convex dependence on the volume V. Whenever such an indication of a first-order phase transition was found, the densities of the coexisting phases were determined by equating the pressures and chemical potentials in both phases using the standard double-tangent construction. The critical temperature of the solid–solid coexistence curve was estimated to be the point where the free-energy curve first developed an inflection point. Of course, this estimate is likely to depend somewhat on the system size. Moreover, the analytical form of equation (4) forces the classical (mean-field) critical behaviour on the solid–solid binodal. We have not attempted to study the true critical behaviour of the solid–solid transition.

Although the solid–solid transition coexistence curves can be obtained from simulations, we have yet to demonstrate that this transition involves phases that are thermodynamically stable. In particular, the melting transition might pre-empt the solid–solid phase separation. It is therefore essential to study the fluid–solid transition as well. We computed the solid–fluid coexistence curve by means of thermodynamic integration. The Helmholtz free energies of the square-shoulder solid and fluid were calculated according to equation (2) using data from our simulations in combination with the known free energies of the hard-sphere reference fluid [17] and solid [16]. For the simulation of both the fluid and the solid, we used a system of 108 square-shoulder spheres in a periodic cubic box. The density was varied from $\rho = 0.8$ to $\rho = 1.04$ in the fluid and from $\rho = 0.9$ to $\rho = 1.2$ in the solid phase. The shoulder width ranged from $\delta = 0.01$ to $\delta = 0.08$. The simulation parameters were equal to those chosen for the simulations of the high-density solid. In the case of

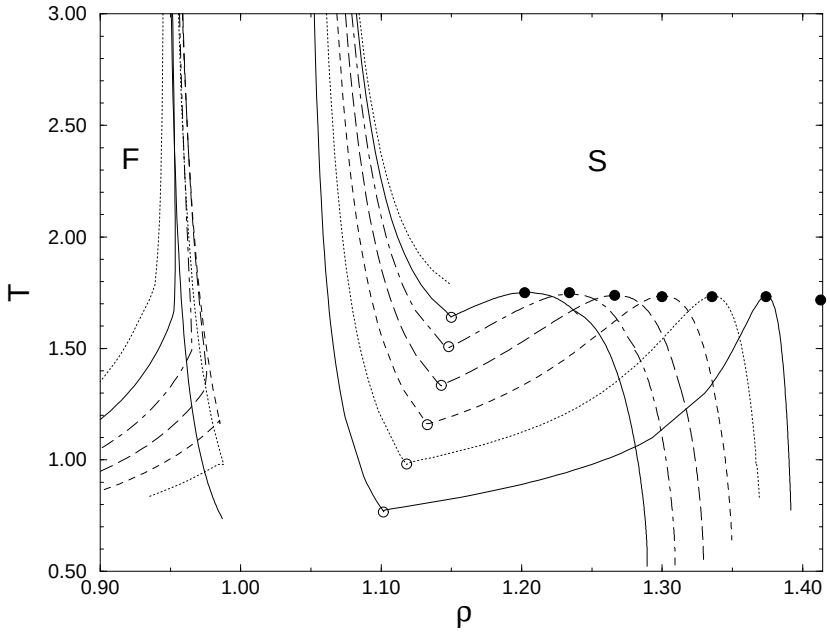

Figure 3. Computed phase diagrams in the T, ρ plane for the fcc structure of 108 square-well particles [2]. Starting with the coexistence curve on the right, from right to left the curves correspond to the well widths $\delta/\sigma = 0.01, 0.02, 0.03, 0.04, 0.05$ and 0.06. The upper dashed fluid–solid coexistence curve refers to a well width of $\delta/\sigma = 0.07$ and shows that the solid–solid transition has become metastable at this point. The critical points are indicated by filled circles, the triple points by open circles. The critical point at $\rho = \sqrt{2}$, corresponding to $\delta/\sigma = 0$, was computed using the lattice model described in reference [2].

a solid we started with an expanded close-packing configuration whereas for the fluid an initial random configuration was compressed to the required density. All of the simulations were equilibrated for 20 000 cycles before data was collected in a production run of 20 000 cycles. To calculate the fluid–solid coexistence one needs the absolute free energy of both the reference fluid and the reference solid phase. The free energy of the hard-sphere fluid was calculated using the accurate Carnahan–Starling equation of state [17], whereas the Hall equation of state [16] was used in the solid region together with an absolute free-energy value obtained from simulations by Frenkel and Ladd [18]. Using these reference free energies and the simulated average internal energies in equation (2) we were able to obtain the coexistence curves for the fluid–solid transition.

Figure 2 shows the computed square-shoulder phase diagrams for $\delta = 0.01, 0.03$ and 0.08. As the simulations did not extend below $T = 0.5$, we extrapolated the binodals to zero temperature. For the sake of comparison, we also show the phase diagram for the corresponding square-well model in figure 3 (see reference [2]). The differences between the repulsive and attractive systems are striking:

(1) as expected, the critical densities for the shoulder potential are higher than those for the square-well model;

(2) the solid–solid binodals go all the way to $T = 0$, where effectively two close-packed solids of hard spheres are in coexistence with each other: one in which the diameter of spheres corresponds to $\sigma + \delta$ and a second with a hard-sphere diameter σ;

(3) the fluid–solid coexistence region changes gradually from the σ hard-sphere case at $T = \infty$ to the $\sigma + \delta$ hard-sphere case at $T = 0$.

Extrapolation of the critical density to larger values of δ leads to the estimate that the solid–solid transition will become metastable with respect to the fluid–solid transition at $\delta \approx 0.25$. Note that this critical value of δ is much larger than for the square-well case. The fact that solid–solid transitions are much more robust for shoulder potentials than for attractive well systems suggests that it may be easier to observe such transitions experimentally in colloidal systems with an effective shoulder potential. This holds not only for the solid–solid phase transition as such, but also for the hexatic phase that is induced by the solid–solid transition in two-dimensional systems [7, 19]. An added advantage of the repulsive-shoulder-potential colloids is that they are less likely to form a gel that will prevent crystallization.

Acknowledgments

The work of the FOM Institute is part of the research programme of the FOM and is made possible by financial support from the Netherlands Organization for Scientific Research (NWO). We thank George Stell for stimulating us to study the repulsive-shoulder-potential model. We gratefully acknowledge discussions with Hartmut Löwen and Luis Mederos. We thank Stuart Rice for sending us preprints of reference [8] and Ignacio Pagonabarraga for a critical reading of the manuscript.

References

[1] Hemmer P C and Lebowitz J L 1976 *Critical Phenomena and Phase Transitions* vol 5b, ed C Domb and M S Green (New York: Academic)
[2] Bolhuis P G and Frenkel D 1994 *Phys. Rev. Lett.* **72** 2211
Bolhuis P G, Hagen M H J and Frenkel D 1994 *Phys. Rev.* E **50** 4880
[3] Tejero C F, Daanoun A, Lekkerkerker H N W and Baus M 1994 *Phys. Rev. Lett.* **73** 752
[4] Daanoun A, Tejero C F and Baus M 1994 *Phys. Rev.* E **50** 2913
[5] Rascon C, Navascués G and Mederos L 1995 *Phys. Rev.* B **51** 14 899
[6] Likos C N, Németh Zs T and Löwen H 1994 *J. Phys.: Condens. Matter* **6** 10 965
[7] Bladon P and Frenkel D 1995 *Phys. Rev. Lett.* **74** 2519
[8] Marcus A H and Rice S A 1996 *Phys. Rev. Lett.* **77** 2577
[9] Jayaraman A 1965 *Phys. Rev.* **137** A179
[10] Stell G and Hemmer P C 1972 *J. Chem. Phys.* **56** 4274
[11] Alder B and Young D 1979 *J. Chem. Phys.* **70** 473
[12] Kincaid J M, Stell G and Goldmark E 1976 *J. Chem. Phys.* **65** 2172
[13] Poole P H, Sciortino F, Grande T, Stanley H E and Angell C A 1994 *Phys. Rev. Lett.* **73** 1632
[14] Mederos L 1996 private communication
[15] Frenkel D and Smit B 1996 *Understanding Molecular Simulation: from Algorithms to Applications* (Boston, MA: Academic)
[16] Hall R 1972 *J. Chem. Phys.* **57** 2252
[17] Carnahan N F and Starling K E 1969 *J. Chem. Phys.* **51** 635
[18] Frenkel D and Ladd A J C 1984 *J. Chem. Phys.* **81** 3188
[19] Chou T and Nelson D R 1996 *Phys. Rev.* E **53** 2560